Journal of Hazardous Materials 398 (2020) 122871

Contents lists available at ScienceDirect

Journal of Hazardous Materials

journal homepage: www.elsevier.com/locate/jhazmat

Glyphosate-dependent effects on photosynthesis of *Solanum lycopersicum* L.—An ecophysiological, ultrastructural and molecular approach

Cristiano Soares[a,*], Ruth Pereira[a], Maria Martins[a], Paula Tamagnini[b,c,d], João Serôdio[e], José Moutinho-Pereira[f], Ana Cunha[g,h], Fernanda Fidalgo[a]

[a] GreenUPorto - Sustainable Agrifood Production Research Centre, Department of Biology, Faculty of Sciences of University of Porto, Rua do Campo Alegre s/n, 4169-007 Porto, Portugal
[b] Bioengineering and Synthetic Microbiology Group, i3S - Instituto de Investigação e Inovação em Saúde, University of Porto, Porto, Portugal
[c] IBMC – Instituto de Biologia Celular e Molecular, University of Porto, Porto, Portugal
[d] Biology Department, Faculty of Sciences of University of Porto, Rua do Campo Alegre s/n, 4169-007 Porto, Portugal
[e] Biology Department and CESAM – Centre for Environmental and Marine Studies, University of Aveiro, Campus de Santiago, 3810-193 Aveiro, Portugal
[f] CITAB - Centre for the Research and Technology of Agro-Environmental and Biological Sciences, Universidade de Trás-os-Montes e Alto Douro, 5000-801 Vila Real, Portugal
[g] Biology Department & CITAB - Centre for the Research and Technology of Agro-Environmental and Biological Sciences, School of Sciences, University of Minho, Campus de Gualtar, 4710-057 Braga, Portugal
[h] CEB – Centre of Biological Engineering, University of Minho, 4710-057 Braga, Portugal

GRAPHICAL ABSTRACT

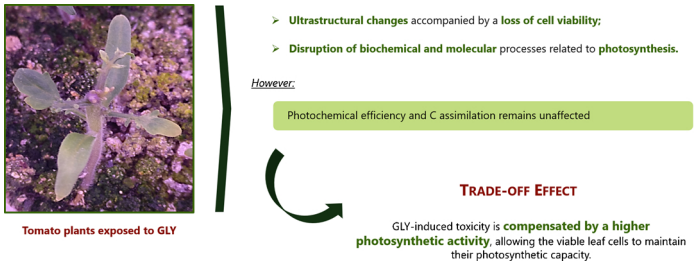

ARTICLE INFO

Editor: D. Aga

Keywords:
Non-target plants
Abiotic stress
Photochemistry
Calvin cycle
Chlorophyll fluorometry
Gas-exchange

ABSTRACT

This study aimed to assess the toxicity of glyphosate (GLY; 0, 10, 20 and 30 mg kg^{-1}) in *Solanum lycopersicum* L., particularly focusing on the photosynthetic metabolism. By combining ecophysiological, ultrastructural, biochemical and molecular tools, the results revealed that the exposure of tomato plants to GLY led to alterations in leaf water balance regulation [increasing stomatal conductance (g_s) and decreasing water use efficiency (WUE_i) at higher concentrations] and induced slight alterations in the structural integrity of cells, mainly in chloroplasts, accompanied by a loss of cell viability. Moreover, the transcriptional and biochemical control of several photosynthetic-related parameters was reduced upon GLY exposure. However, *in vivo* chlorophyll fluorometry and IRGA gas-exchange studies revealed that the photosynthetic yield of *S. lycopersicum* was not repressed by GLY. Overall, GLY impacts cellular and subcellular homeostasis (by affecting chloroplast structure, reducing photosynthetic pigments and inhibiting photosynthetic-related genes transcription), and leaf structure, but is not

* Corresponding author.
E-mail address: cfsoares@fc.up.pt (C. Soares).

https://doi.org/10.1016/j.jhazmat.2020.122871
Received 16 October 2019; Received in revised form 24 April 2020; Accepted 4 May 2020
Available online 14 May 2020

reducing the carbon flow on a leaf area basis. Altogether, these results suggest a trade-off effect in which GLY-induced toxicity is compensated by a higher photosynthetic activity related to GLY-induced dysfunction in g_s and an increase in mesophyll thickness/density, allowing the viable leaf cells to maintain their photosynthetic capacity.

1. Introduction

As a result of the accelerated world population growth, as well as of the increased food and feed demands, agriculture is progressively more dependent on the use of chemical products to ensure high yield rates. According to recent data, pesticide application, increasing since 1990, has surpassed, on average, the mark of 2.5 kg ha^{-1} worldwide and it is expected that this value will be further aggravated in the following years (http://www.fao.org/faostat/en/#data/EP/visualize). From all pesticide classes, herbicides and insecticides are currently the most representative ones, accounting for the highest production volume (Atwood and Paisley-Jones, 2017). Among all herbicides, glyphosate [GLY; N-(phosphonomethyl) glycine] is the most used at the global scale, with global application rates exceeding 820 million kg between 1998 and 2014 (https://www.statista.com/statistics/567250/glyphosate-use-worldwide/).

GLY is considered as a broad-spectrum herbicide of systemic and non-selective action, commonly applied to leaves of weeds (Franz et al., 1997). Regarding its mode-of-action, GLY inhibits the activity of the 5-enolpyruvylshikimate-3-phosphate synthase (EPSPS; EC 2.5.1.19), blocking the shikimate pathway and consequently the biosynthesis of aromatic amino acids and secondary metabolites in plants and some species of microorganisms (Franz et al., 1997). Due to its low price, great efficacy, along with the development of several GLY-resistant species, such as maize and soybean transgenic cultivars, GLY rapidly turn into the most used herbicide worldwide. Additionally, GLY became regarded as the most innocuous option of weed chemical control for the environment, since, once in contact with the soil, it quickly degrades (DT50 in the field = 23.79 days, http://sitem.herts.ac.uk/aeru/iupac/Reports/373.htm) into aminomethyl phosphonic acid (AMPA). However, GLY can remain adsorbed to clay and organic matter, lowering its degradation rates, which are also highly dependent on soil pH (Zhang et al., 2015). All of these factors can potentiate GLY, as well as AMPA, accumulation in the soil (see review by Van Bruggen et al. (2018)), where they can persist or move to other environmental compartments. Although there are still few studies reporting the accumulation, fate and transport of GLY and of its degradation products in soils, especially in EU countries (Silva et al., 2018), residual levels of GLY and AMPA have been detected up to μg kg^{-1} and mg kg^{-1}, reaching values up to 8 mg kg^{-1} in agricultural soils (Costa et al., 2017; Peruzzo et al., 2008). Besides, since GLY residues in surface waters have also reached 15 mg L^{-1} (Wei et al., 2016), it is expected that soil can present even higher amounts due to repetitive applications (Soares et al., 2019a). Thus, given the widespread use of GLY-based herbicides, along with data confirming its accumulation in the environment, there is a growing need to adequately evaluate its potential toxicity to non-target biota. Within this context, in the past few years, scientific evidence has been showing that GLY is not as safe as it was thought to be, being able to negatively affect the environment, either directly or through the production of AMPA, which is also toxic (Bai and Ogbourne, 2016; Borggaard and Gimsing, 2008). Indeed, there is currently a strong debate on this matter amongst the scientific community, since contrasting and divergent data in relation to GLY's non-target effects have been reported, especially on animal species, including mammals (Silva et al., 2018). For instance, the World Health Organization has classified GLY as potential carcinogenic, but, in 2017, the United States Environmental Protection Agency (US-EPA) stated that GLY does not represent a risk to the human health, with no evidence that GLY is carcinogenic (EPA, 2017). Despite the great number of studies in animals, not much is known regarding the responses of non-target plants to GLY exposure through contaminated soils/waters. Given the high application rates of GLY, this aspect is quite concerning, since contaminated soils can be unable to grow crops, as well as other important plant species. In this way, new studies addressing this issue under realistic and ecologically relevant concentrations of GLY are of special importance to identify the main effects of the environmental contamination by GLY on the growth and development of crops, produced for both human and animal feeding. Recent research unequivocally indicated that the presence of high levels of GLY greatly impaired the growth and performance of non-target plant species (Soares et al., 2019a; Gomes et al., 2017; Spormann et al., 2019), affecting multiple biological mechanisms, from the oxidative metabolism to cellular respiration and photosynthesis (Gomes et al. (2014) and references therein).

From all the processes occurring in a plant cell, photosynthesis is crucial to ensure the cellular homeostasis necessary to the normal plant development (Taiz et al., 2015). Effects on photosynthesis may thus have major impact on plant productivity, and recent reports have shown that it is seriously affected by herbicides (Sharma et al., 2018; Parween et al., 2016). Although GLY's mode-of-action does not directly block the photosynthetic mechanism, some authors advocate that this herbicide can affect photosynthesis (Mateos-Naranjo et al., 2009; Zobiole et al., 2012; Yanniccari et al., 2012), both indirectly, by preventing the biosynthesis of chlorophylls by the action of AMPA, and directly, by enhancing chlorophyll degradation (2014). However, using chlorophyll fluorescence approaches, inhibitory effects of GLY on the photosystem II (PSII) activity, electron transport rate (ETR) and non-photochemical quenching (NPQ) were documented (see review by Gomes et al. (2014)). Yet, in the great majority of these studies, GLY was applied on leaves, thus not translating potential effects on non-target plant species exposed to GLY by soil contamination.

Tomato plant (*Solanum lycopersicum* L.) is one of the main agricultural crop species produced worldwide, being also considered as the second most important vegetable, not only due to its excellent nutritional properties, but also to its antioxidant and health-promoting characteristics (Dorais et al., 2008; Branco-Neves et al., 2017). Besides its economic importance, tomato is also acknowledged for being a perfect model species for plant stress physiology studies (Gerszberg et al., 2015). Although *S. lycopersicum* is not directly exposed to GLY, since it is a non-target plant species, the environmental contamination by this herbicide may end up affecting tomato plants' growth, development and survival. Actually, a recent work from our group revealed that realistic levels of GLY in the soil greatly impair tomato growth, by inducing severe oxidative damage in both shoots and roots after 28 days of growth (Soares et al., 2019a). However, to the best of our knowledge, no study on the interplay between GLY contamination and the carbon (C) metabolism on non-target plants has been reported so far. In this context, the main goal of this work was to evaluate the effects of soil contamination by GLY, provided as RoundUp® UltraMax, on C assimilation and photosynthetic efficiency of *S. lycopersicum* L. Since photosynthesis is a very complex mechanism, involving several processes from gene expression, protein synthesis and enzyme activity, to photoprotective and damage repair mechanisms, at the cellular level, and to gas diffusion, at the leaf level, different methodologies were employed to unveil the mechanism of action of this herbicide and its subsequent effect on non-target plants. For this purpose, 28-days soil grown seedlings exposed to increasing concentrations of GLY (0, 10, 20 and 30 mg kg^{-1}) were used to evaluate: i) the content of photosynthetic pigments and RuBisCO, ii) the ultrastructure of mesophyll cells and

histochemical detection of cell death, iii) *in vivo* photosynthetic performance by chlorophyll fluorescence and infrared-gas analyses, and iv) the expression level of several photosynthetic-associated genes.

2. Materials and methods

2.1. Chemicals and substrate

The herbicide Roundup®UltraMax (Monsanto Europe, S.A., Belgium), a GLY-based (360 g L^{-1}, potassium salt) herbicide, acquired from a local supplier, was used to prepare a stock solution of 1 g L^{-1}, which was then diluted to achieve the tested concentrations (10, 20 and 30 mg kg^{-1} soil). The substrate used to grow plants was an artificial soil [pH 6.0 ± 0.5, 5% (w/w) organic matter], composed by sphagnum peat, quartz sand (< 2 mm) and kaolin clay (OECD, 2006).

2.2. Plant material and germination conditions

Seeds of *S. lycopersicum* L. cv. Micro-Tom, obtained from FCUP seed collection, were surface disinfected with 70% (v/v) ethanol, followed by 20% (v/v) commercial bleach [5% (v/v) active chlorine], containing 0.05% (w/v) Tween-20, for 7 min each, followed by a series of cleanup with distilled deionized water (ddH_2O). Seeds were then placed in Petri plates containing half-strength MS medium (Murashige and Skoog, 1962) solidified with 0.625% (w/v) agar and left to germinate in a growth chamber under controlled conditions (photoperiod: 16 h light/8 h dark; temperature: 25 ± 1 °C; photosynthetic photon flux density (PPFD): 150 µmol m^{-2} s^{-1}).

2.3. Experimental setup

At day 8, sets of six plantlets were transferred to plastic pots containing 200 g soil. After determining the maximum water hold capacity (WHC_{max}) of the soil, the volume of water required to adjust soils to 40% of its WHC was used to dilute GLY stock solution to attain the final concentrations of 10, 20 and 30 mg kg^{-1} soil. A control with no GLY (CTL; 0 mg kg^{-1}) was also included. The concentrations herein used were selected based on a recent work of our group (Soares et al., 2019a) and are all environmentally relevant, as previously demonstrated. For each treatment, four replicates (pots) were prepared, with six plants each. At the beginning of the assay, to ensure the availability of mineral nutrients, 100 mL of Hoagland solution (Taiz et al., 2015) (pH 5.8) were added to a box placed under each pot, communicating by a cotton rope, and plants were grown for 5 weeks under the same conditions as described above and irrigated with ddH_2O when necessary. At the end of this period, fully expanded leaves (2nd and 3rd) were randomly collected from three plants of each biological replicate, randomly selected, and frozen under liquid nitrogen (N_2) for subsequent biochemical and molecular analyses or immediately processed for transmission electron microscopy (TEM). All the other *in vivo* parameters were measured in fully expanded leaves from at least two plants from each biological replicate.

2.4. Biochemical assays—photosynthetic pigments and relative RuBisCO content

Total chlorophylls (Chl a + b) and carotenoids (Car) were extracted from frozen leaf samples (ca. 100 mg) with 80% (v/v) acetone. After centrifugation (1400*g*; 10 min) for clearing the extract, the absorbance (Abs) was recorded at 663, 647 and 470 nm, and Chl *a* + *b* and Car contents determined using Lichtenthaler (1987) equations.

Ribulose-1,5-bisphosphate carboxylase/oxygenase (RuBisCO; EC 4.1.1.39) relative content was quantified as in Soares et al. (2016a), from a protocol originally described by Li et al. (2013). Briefly, after protein extraction and quantification (Bradford, 1976), 20 µg of extract from each biological replicate were loaded onto a polyacrylamide gel and separated by electrophoresis under denaturing conditions. Then, following gel staining with BlueSafe (NZYTech©), the portions of the large and small subunits of RuBisCO of each sample were excised and incubated in formamide at 50 °C overnight. The remaining gel was also incubated under the same conditions. Lastly, the Abs of the washing solution was measured at 595 nm and the relative RuBisCO levels expressed according to a mathematical formula (Soares et al., 2016b).

2.5. Histochemical detection of cell viability

Cell viability of tomato leaves was evaluated as described in Soares et al. (Soares et al., 2016a). After 4 h-incubation in dark conditions in 0.25% (w/v) Evans Blue, leaves were boiled in 96% (v/v) ethanol for pigment decolorization, then, carefully rinsed with deionized water and photographed. The presence of blueish spots in the leaf is an indicator of the cell death.

2.6. Gene expression analysis by RT-qPCR

2.6.1. RNA extraction and cDNA synthesis

Total RNA was extracted from leaf tissue (ca. 80 − 100 mg) with NZYol® reagent (NZYTech, Lda) according to, the guidelines of the manufacturer. After extraction, RNA was spectrophotometrically quantified at 260 nm in a µDrop Plate (Thermo Fisher Scientific) and its integrity assessed by 0.8% (w/v) agarose gel electrophoresis. Each RNA sample was treated with ezDNase enzyme (Invitrogen) to prevent any genomic DNA contamination. Then, cDNA synthesis was performed with SuperScript™ IV VILO™ Master Mix, using 2.5 µg RNA in a final volume of 20 µL. At the end, cDNAs were diluted (1:10) and stored at − 20 °C for real-time PCR expression analysis.

2.6.2. Real-time PCR (qPCR) conditions and primers

cDNA from each experimental condition was amplified through qPCR in a CFX96 Real-Time Detection System (Bio-Rad®, Portugal), using the specific primers listed in Table 1. All qPCR reactions were performed in triplicate, using PowerUp™ SYBR™ Green Master Mix (Applied Biosystems) for a final volume of 20 µL, containing 1 µL of diluted cDNA. The qPCR conditions were as follow: 2 min at 50 °C, 2 min at 95 °C, followed by 35 cycles of 3 s at 95 °C and 30 s at 60 °C. At the end of each reaction, a melting curve was carried out by gradually

Table 1
Gene-specific primers used in q-PCR analysis.

Gene name	Primer sequence	Tm (ºC)	Amplicon (bp)	Reference
D1	Fwd: 5- TGG ATG GTT TGG TGT TTT GAT G -3 Rev: 5- CCG TAA AGT AGA GAC CCT GAA AC -3	Fwd: 54.03 Rev: 54.83	191	Mariz-Ponte, 2017)
CP47	Fwd: 5- CCT ATT CCA TCT TAG CGT CCG -3 Rev: 5- TTG CCG AAC CAT ACC ACA TAG -3	Fwd: 54.90 Rev: 54.87	142	Mariz-Ponte, 2017)
RCBL	Fwd: 5- ATC TTG CTC GGG AAG GTA ATG -3 Rev: 5- TCT TTC CAT ACC TCA CAA GCA G -3	Fwd: 54.68 Rev: 54.64	81	Mariz-Ponte, 2017)
RCBS	Fwd: 5- TGA GAC TGA GCA CGG ATT TG -3 Rev: 5- TTT AGC CTC TTG AAC CTC AGC -3	Fwd: 54.90 Rev: 54.79	148	Mariz-Ponte, 2017)

increasing the temperature from 60 to 95 °C in 0.5-s intervals, in order to ensure primer and amplification specificity. For normalization of the expression data, four reference genes previously validated and tested were used (*18S* – (Leclercq et al., 2002); *UBI* and *ACTIN* – (Løvdal and Lillo, 2009); *EF1* – Dzakovich et al., 2016) and the quantification of the transcript levels was executed by applying the $2^{\Delta\Delta Ct}$ method (Livak and Schmittgen, 2001).

2.7. Ultrastructure analysis by TEM

Leaf samples were fixed in a mixture of 5% (v/v) glutaraldehyde and 4% (v/v) paraformaldehyde (PFA) and post-fixed in 2% (w/v) osmium tetroxide (OsO_4), prepared in 0.1 M sodium cacodylate buffer (pH 7.2). Then, dehydration was carried out using increased concentrations of ethanol, followed by embedding in EMBed-812. Finally, ultrathin sections were obtained using a ultramicrotome, contrasted with uranyl acetate and lead citrate, and observed using a Zeiss EM C10 TEM (Zeiss, Göttingen, Germany).

2.8. Chlorophyll fluorescence analyses

2.8.1. Photochemical efficiency of PSII—F_v/F_m, ϕPSII and rETR

Chlorophyll fluorescence analysis, by pulse amplitude modulated fluorometry (PAM), was performed in the 2nd and 3rd young fully expanded leaves of tomato plants, using a PAM-210 fluorometer (Heinz Walz GmbH, 1997), controlled via the PAMWin software. The emitter-detector unit comprises a red measuring light LED with short-pass filter (< 690 nm), peaking at ca. 650 nm, an actinic red LED (unfiltered, peaking at ca. 665 nm), a far-red LED, with a long-pass filter (> 710 nm, peaking at ca. 730 nm), and a PIN photodiode and dichroic filter, reflecting fluorescence at 90° towards the detector. Prior to the measurements, plants were dark-adapted for at least 20 min to open all the PSII reaction centers. Then, after recording the minimal fluorescence (F_0), a saturating light pulse (3500 µmol photons m^{-2} s^{-1}, 800 ms) was applied to determine the maximal fluorescence yield (F_m) and calculate the maximum quantum yield of PSII ($F_v/F_m = (F_m - F_0)/F_m$; (Kitajima and Butler, 1975)). In order to estimate the effective quantum yield of PSII ($\Phi PSII = (F'_m - F_t)/F'_m$; (Genty et al., 1989)) and the respective relative electron transport rate (rETR = ΦPSII x PPFD; (Genty et al., 1989)), indicative of the electrons pumped through the photosynthetic chain under plant growth light conditions, leaves were adapted for 5 min to actinic light (AL; 128 µmol photons m^{-2} s^{-1}) and, then, a saturating pulse was applied to record F'_m and F_t.

2.8.2. Photochemical efficiency recovery study

After the screening of the photosynthetic yield of tomato leaves of plants under GLY contamination, a new PAM chlorophyll fluorometry-based study was designed to investigate GLY effects on the non-photochemical quenching efficiency and F_v/F_m recovery of tomato leaves. All the experiments were performed using an imaging chlorophyll fluorescence fluorometer (FluorCAM 800 M F, Photon System Instruments, Brno, Czech Republic), comprising a control unit (SN-FC800-082, PSI) and a CCD camera (CCD381, PSI) with a f1.2 (2.8–6 mm) objective (Eneo, Japan). Multiple samples were exposed simultaneously to actinic light, by using an LCD digital projector (EB-X14; Seiko Epson, Suwa, Japan), controlled as described Serôdio et al. (2017). Briefly, five leaf discs (≈2 cm) from each experimental condition were placed on the surface of 2 mL of water in a 24-well microplate. After 20 min of dark adaptation, F_v/F_m was measured as described above, and samples were exposed to saturating AL (1800 – 2100 µmol m^{-2} s^{-1}) for 1 h. A saturating light pulse was then applied to record F_m' and calculate the non-photochemical quenching [$NPQ = (F_m - F'_m)/F'_m$], which corresponds to the fraction of light captured by Chl that is converted into heat (Genty et al., 1989). Afterwards, the AL was switched off and saturating pulses were provided every 3 min to evaluate F_v/F_m recovery. Images of chlorophyll

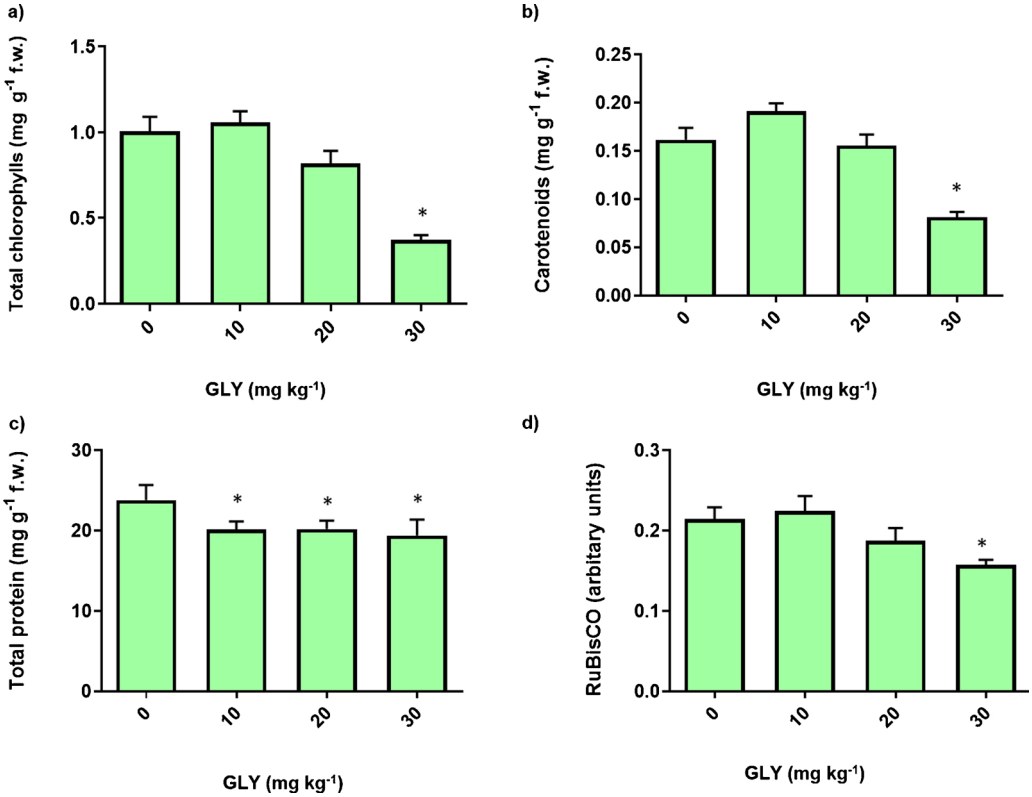

Fig. 1. Total chlorophylls (a), carotenoids (b), total protein (c) and RuBisCO (d) levels in leaves of *S. lycopersicum* plants exposed to increased concentrations (0, 10, 20 and 30 mg kg^{-1}) of GLY. *Above bars indicate differences from the CTL (0 mg kg^{-1}) at $p \leq 0.05$.

fluorescence parameters were captured by applying modulated measuring light (< 0.1 μmol m^{-2} s^{-1}) and saturation pulses (> 7500 μmol m^{-2} s^{-1}) provided by red (612 nm emission peak, 40 nm bandwidth) LED panels. Images (512 × 512 pixels) were processed using FluorCam7 software (Photon System Instruments). The results were expressed as the proportion of F_v/F_m recovery in relation to the original value.

2.9. Gas exchange measurements

The evaluation of gas-exchange parameters was performed using an infrared gas analyzer (IRGA; *LC pro+*, ADC, Hoddersdon, UK), coupled to a broad light source (PPFD of 255 μmol m^{-2} s^{-1}), simulating the greenhouse conditions (atmospheric CO_2 concentration and a PPFD of 120 μmol photons m^{-2} s^{-1}). For each of the four replicates, measurements were made in two plants, being each measurement repeated twice to assess the feasibility of the method. Net CO_2 assimilation rate (P_N, μmol m^{-2} s^{-1}), stomatal conductance (g_s, mmol m^{-2} s), transpiration rate (E, mmol m^{-2} s^{-1}), and intercellular CO_2 concentration (C_i, μmol mol^{-1}) were estimated using the equations developed by von Caemmerer and Farquhar (von Von Caemmerer and Farquhar, 1981). Intrinsic water use efficiency (WUE_i) was determined as follows: $WUE_i = P_N/g_s$. In complement, the specific leaf area [SLA = leaf area (cm^2)/dry mass (g)] was also calculated.

2.10. Statistical analysis

All biochemical, molecular and physiological evaluations were performed using four experimental replicates (n = 4), except for the ultrastructure analysis where n = 2 was considered. The results were expressed as mean ± standard error of the mean (SEM). The effect of different GLY concentrations on the parameters assessed were analyzed by one-way ANOVA, assuming a significance level of 0.05, after checking for the normality and homoscedasticity assumptions. Whenever significant differences ($p \leq 0.05$) were found, Dunnet *post-hoc* tests were used to identify differences between each GLY treatment – 10, 20 and 30 mg kg^{-1} – and the CTL. Correlation analyses were performed using Spearman's test. All statistical procedures were executed in Prism 8 (© 2018 GraphPad Software).

3. Results

3.1. Biochemical determinations—photosynthetic pigments, soluble protein and RuBisCO

As shown in Fig. 1, Chl $a + b$ (Fig. 1a) and carotenoid contents significantly decreased [Chl $a + b$ –F (3, 10) = 24; $p < 0.01$; Car – F (3, 11) = 21.03; $p < 0.01$] when tomato plants were exposed to the highest GLY concentration (30 mg GLY kg^{-1}) (Dunnet: $p < 0.05$) to about 40 and 50% of the control, respectively.

Total soluble protein levels were also significantly reduced [F (3, 11) = 9.399; $p = 0.0023$] under GLY exposure, with significant changes from the control detected for all concentrations of GLY (Dunnet: $p < 0.05$), even in the lowest one (10 mg GLY kg^{-1}) (Fig. 1c). Again, a GLY effect was detected in the relative content of RuBisCO [F (3, 12) = 4.345; $p < 0.015$] (Fig. 1d). Although a dose-dependent inhibition was apparent, significant differences from the CTL were only found when plants were grown at 30 mg kg^{-1} (Dunnet: $p < 0.05$).

3.2. Cell viability assay

The exposure of tomato plants to GLY induced losses in cell viability of leaves, as can be seen in Fig. 2. As the blueish areas are indicative of cell death, it is also clear that this effect was dependent on the concentration of GLY, reaching a maximum in the plants subjected to the highest concentration tested (30 mg kg^{-1}).

3.3. Foliar morphology and ultrastructure analysis by TEM

When tomato plants were grown in the presence of increasing concentrations of GLY, alterations in plant growth, leaf morphology and mesophyll structure were registered. As can be observed in Figs. 3a–b, the compound leaves of GLY-treated plants suffered profound changes, with less primary and secondary leaflets and with more rounded terminal leaflets at the highest concentration tested. The SLA was also significantly reduced [F (3, 23) = 10.76; $p = 0.0001$] upon exposure to the highest GLY concentrations (20 and 30 mg GLY kg^{-1}), to values around 70% of those registered in the CTL (Fig. 3c).

The ultrastructure of tomato leaves exposed to increased concentrations of GLY (0, 10, 20 and 30 mg kg^{-1}) are depicted in Figs. 4–6. As can be observed, mesophyll cells from CTL plants displayed

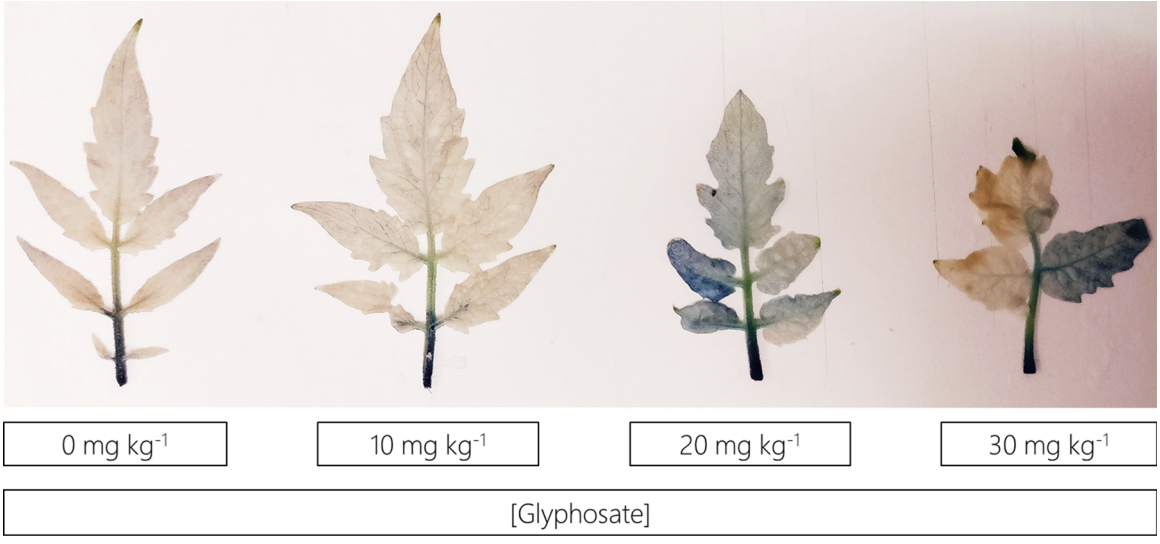

Fig. 2. Histochemical detection of cell death in leaves of *S. lycopersicum* plants exposed to increased concentrations (0, 10, 20 and 30 mg kg^{-1}) of GLY. Necrotic areas are manifested as blue spots on the leaf surface (For interpretation of the references to color in this figure legend, the reader is referred to the web version of this article).

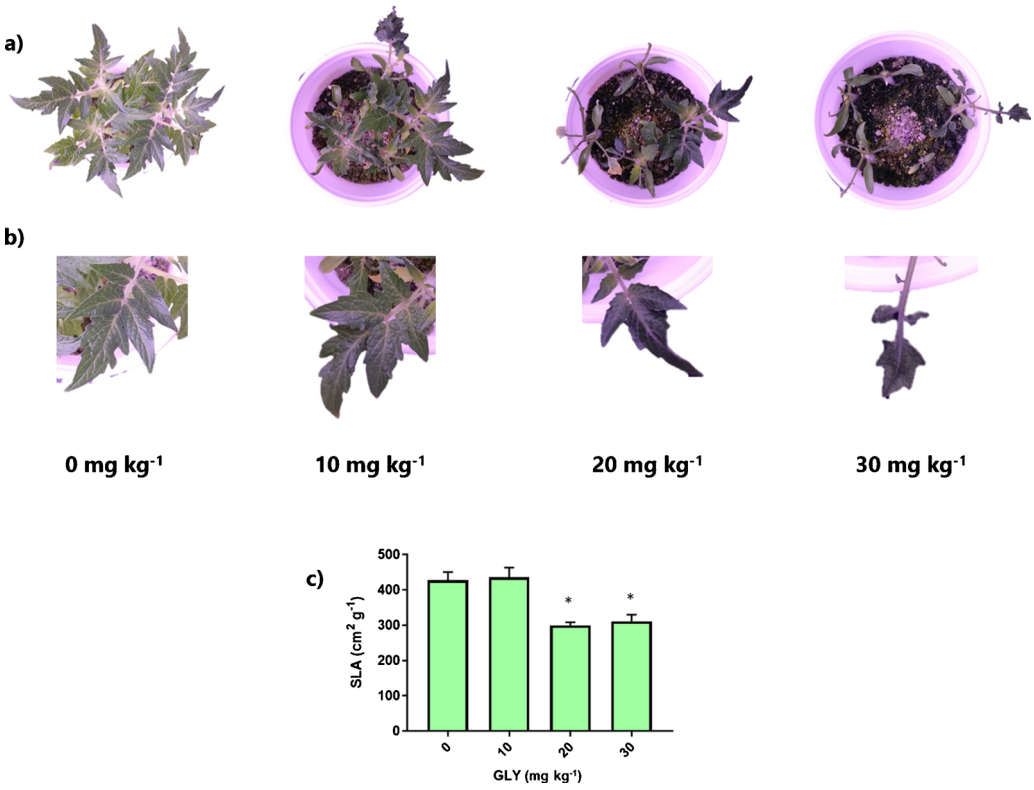

Fig. 3. Growth comparison (a), leaf morphology (b) and specific leaf area (SLA; c) in leaves of *S. lycopersicum* plants exposed to increased concentrations (0, 10, 20 and 30 mg kg^{-1}) of GLY. *Above bars indicate differences from the CTL (0 mg kg^{-1}) at $p \leq 0.05$.

abundant and lens-shaped chloroplasts, with well-organized thylakoid system, along with the accumulation of multiple starch grains (Fig. 4a–b). Other cellular organelles, such as peroxisomes and mitochondria had also their integrity well preserved (Fig. 4c, d). However, upon exposure to GLY, substantial ultrastructural changes occurred in tomato leaves. As illustrated in Figs. 5 and 6, as GLY concentration increases, chloroplasts displayed a variable degree of thylakoid swelling and increased damage in thylakoid membranes organization, though no apparent changes in starch accumulation has been notice. However, the appearance of numerous plastoglobuli (PG) in response to GLY treatments was strongly induced (Figs. 5 and 6a–b), along with an increase of peroxisomes and mitochondria abundance, especially in plants exposed to 30 mg kg^{-1} (Fig. 6a–d).

3.4. Transcriptional regulation of photosynthesis-related genes

The transcript accumulation of genes coding for PSII proteins (D1 and CP47), as well as for the small and large subunits of RuBisCO, was

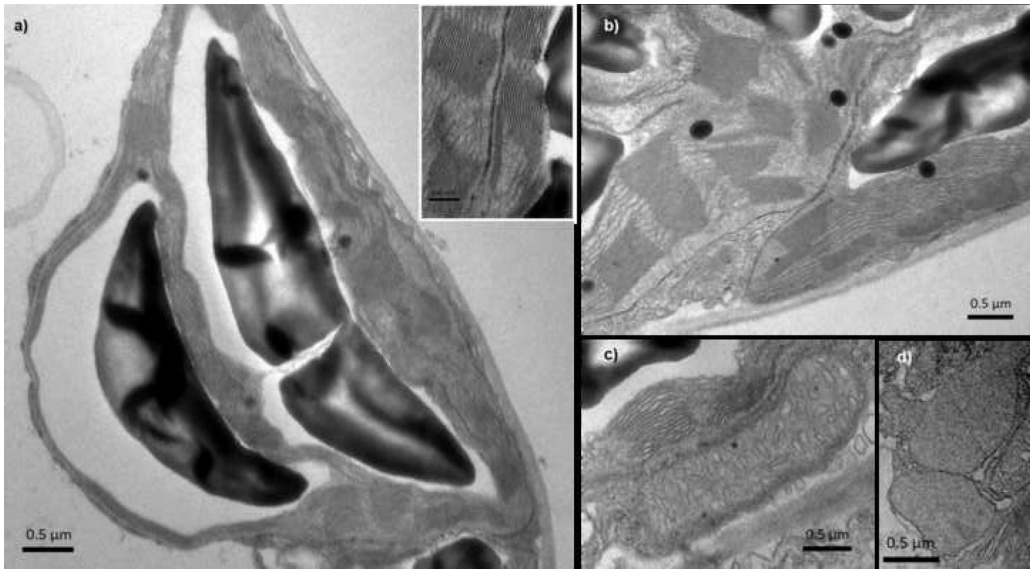

Fig. 4. Ultrastructural analysis of the foliar mesophyll of *S. lycopersicum* plants grown under control conditions (no GLY). (a) Region of a mesophyll cell showing well-preserved chloroplasts, which contain huge starch grains; high magnification of well-preserved chloroplasts (b), mitochondria (c) and peroxisomes (d).

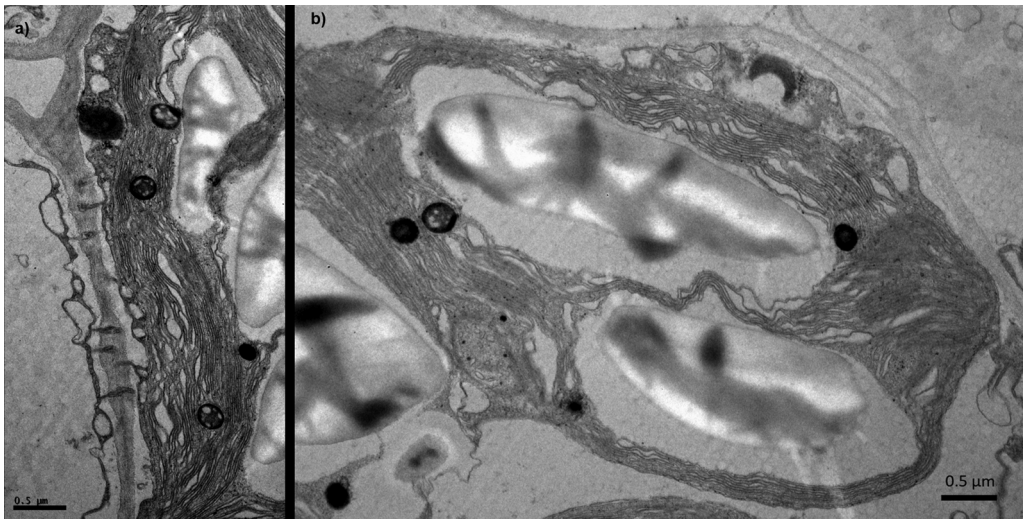

Fig. 5. Ultrastructural analysis of the foliar mesophyll of *S. lycopersicum* plants exposed to 20 mg kg^{-1} (a) portion of a mesophyll cell displaying marked abnormalities in chloroplast ultrastructure, with a higher incidence of osmiophilic deposits (plastoglobuli); (b) Damaged chloroplast, showing swelling thylakoids, with no apparent change in starch accumulation.

evaluated by qPCR (Fig. 7). Upon exposure to GLY, gene expression of D1 and CP47 was strongly repressed in a dose dependent-manner and for all the concentrations tested [D1: ($F(3, 8) = 437.4$; $p < 0.01$ and CP47: ($F(3, 8) = 530.2$; $p < 0.01$], reaching minimal values (up to 15% of the CTL) in plants exposed to 20 and 30 mg GLY kg^{-1} (Dunnet: $p < 0.05$). Concerning genes related to RuBisCO, the expression of *RCBL* [$F(3, 8) = 234.4$; $p < 0.01$] and *RCBS* [$F(3, 8) = 43.28$; $p < 0.01$] was also affected by GLY, but only under the two highest treatments (Dunnet: $p < 0.05$; Fig. 5b).

3.5. Chlorophyll fluorescence analysis

3.5.1. Photochemical and non-photochemical efficiency at plant growth light conditions

GLY induced significant changes in leaf photosynthetic potential quantum yield and photosynthetic activity, as revealed by the results obtained for F_v/F_m [$F(3, 26) = 18.96$; $p < 0.01$], ΦPSII [$F(3, 26) = 36.78$; $p < 0.01$], rETR [$F(3, 28) = 23.49$; $p < 0.01$], and NPQ [$F(3, 24) = 19.96$; $p < 0.01$] (Fig. 8a–d). Actually, after adapting the leaves for 5 min to growth light conditions (AL ≈ 128 µmol m^{-2} s^{-1}), GLY induced a positive response for all the analyzed parameters, significantly increasing ΦPSII (up to 45%; Dunnet: $p < 0.05$) and rETR (up to 45%; Dunnet: $p < 0.05$) and decreasing NPQ (up to 51%; Dunnet: $p < 0.05$) in relation to the CTL, in a concentration-independent manner.

3.5.2. NPQ dark relaxation and F_v/F_m recovery studies

The recovery of the maximum quantum yield following light exposure, expressed as % of the F_v/F_m initial values, is represented in Fig. 9. The results showed that, after 1 h exposure to saturating high light conditions (1800 − 2100 µmol m^{-2} s^{-1}), tomato plants exposed to GLY, especially those under the highest concentrations (20 and

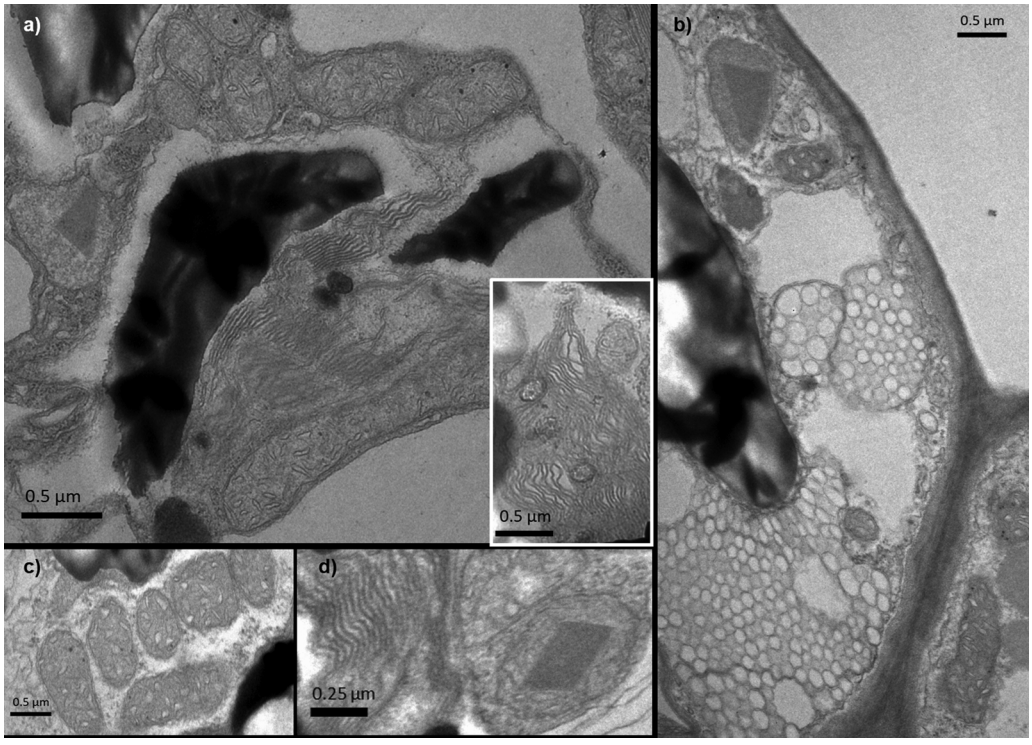

Fig. 6. Ultrastructural analysis of the foliar mesophyll of *S. lycopersicum* plants grown exposed to 30 mg kg^{-1}. (a) Region of a mesophyll cell showing damaged chloroplasts and a huge occurrence of mitochondria. Inset: magnification of thylakoid membrane disorganization; (b) portion of a cell exhibiting signs of great damage, with the appearance of several vesicular bodies throughout the chloroplast; magnification of mitochondria (c) and peroxisome (d) with a paracrystaline inclusion.

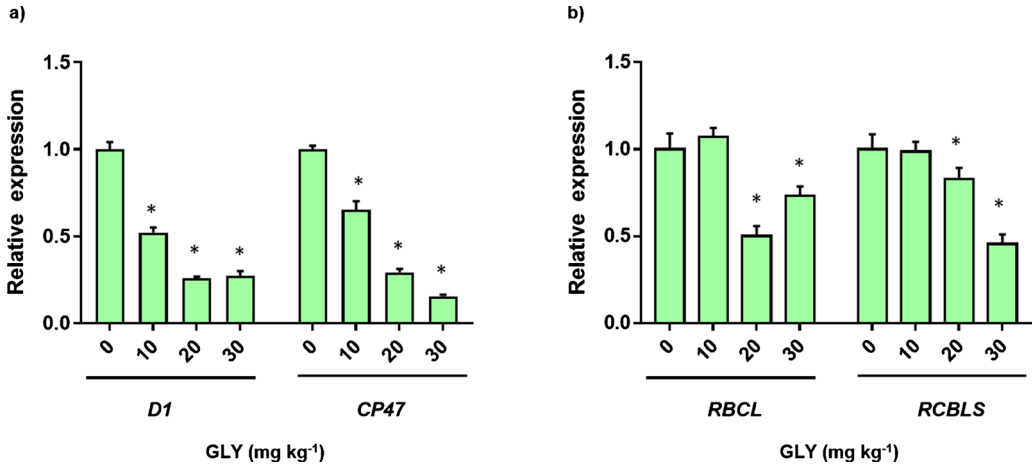

Fig. 7. Expression profile of *D1* and *CP47* (a), and *RBCL* and *RBCS* (b) genes leaves of *S. lycopersicum* plants exposed to increased concentrations (0, 10, 20 and 30 mg kg^{-1}) of GLY. *Above bars indicate differences from the CTL (0 mg kg^{-1}) at $p \leq 0.05$.

30 mg kg^{-1}), were the ones showing the highest F_v/F_m recovery (respectively to 85 and 87% of the initial value), exhibiting a steady increment from minute 6 to the last measure (after 30 min). The CTL plants presented the lowest recoveries, reaching recovery values of only 70%.

3.6. Gas exchange measurements

GLY exposure increased the stomatal conductance (g_s) [F (3, 16) = 37.74; $p < 0.01$] and leaf transpiration (E) [F (3, 18) = 19.20; $p < 0.01$] in a dose-dependent manner, though significant differences from the CTL (Dunnet: $p < 0.05$) were only recorded in plants exposed to the two highest concentrations (Fig. 10a–b). In parallel, GLY treatment also had a significant impact on the net CO_2 assimilation rate (P_N) [F (3, 17) = 149.9; $p < 0.01$], with increases of 2.9 − 2.2-fold in plants exposed to 20 and 30 mg GLY kg^{-1}, respectively (Fig. 8c). No differences were recorded for intracellular concentration of CO_2 (C_i) among groups (Fig. 7d). Regarding the water use efficiency (WUE_i) [F (3, 16) = 31.9; $p < 0.05$], a significant decrease (Dunnet: $p < 0.05$) of about 50% was recorded in plants under the highest concentration of

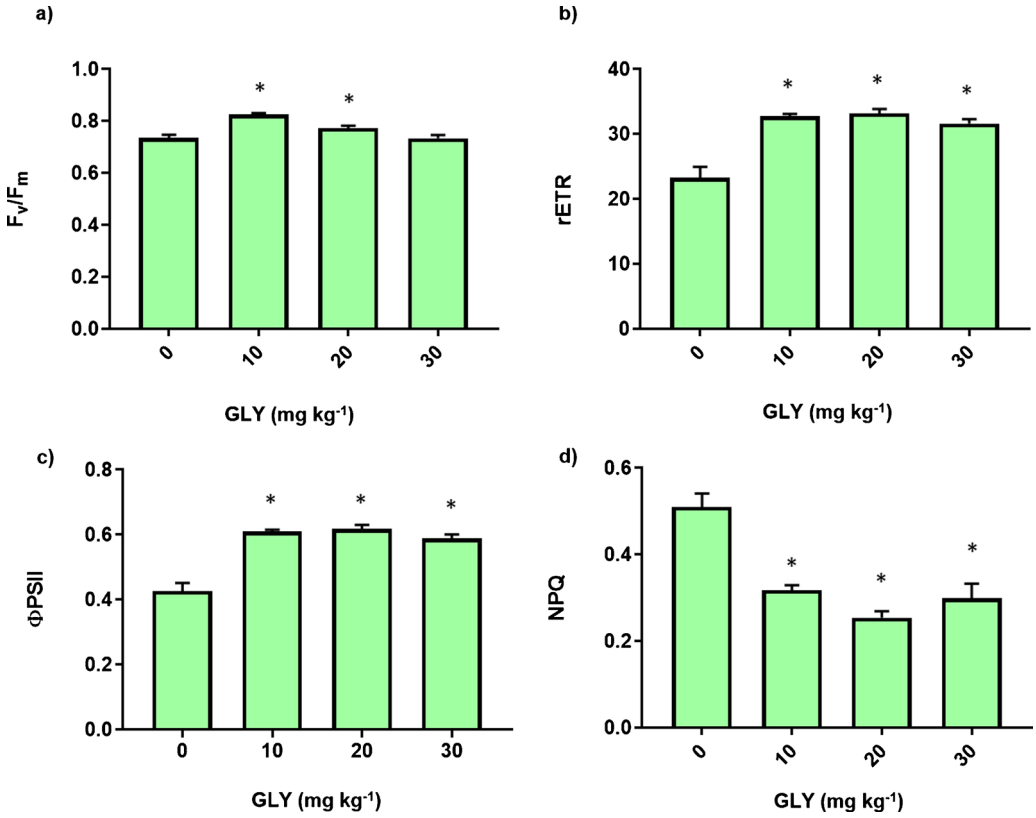

Fig. 8. F_v/F_m (a), ETR (b), ΦPSII (c) and NPQ (d) in leaves of *S. lycopersicum* plants exposed to increased concentrations (0, 10, 20 and 30 mg kg^{-1}) of GLY. *Above bars indicate differences from the CTL (0 mg kg^{-1}) at $p \leq 0.05$.

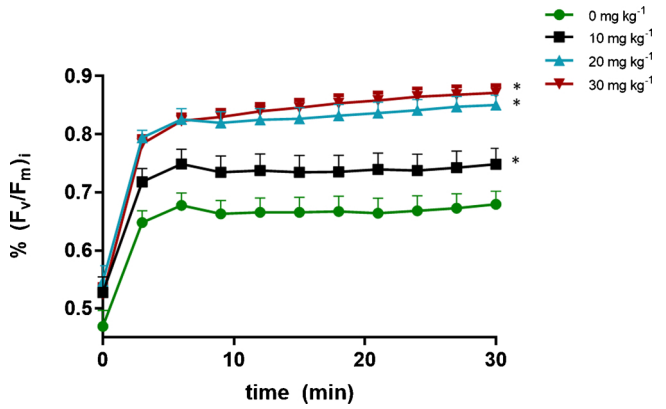

Fig. 9. Photochemical recovery of F_v/F_m, exspressed as % in relation to the initial F_v/F_m value, in leaves of *S. lycopersicum* plants exposed to increased concentrations (0, 10, 20 and 30 mg kg^{-1}) of GLY after 1 h of exposure to saturating AL (≈1800–2100 µmol photons m^{-2} s^{-1}).

GLY, in relation to the CTL (Fig. 10e).

4. Discussion

Due to their sessile nature, plants' growth and development are largely dependent on their adaptability to an ever-changing environment, where they face constant abiotic fluctuations (e.g. water stress, radiation, temperature) and contact with different contaminants, such as pesticide residues in soil and/or irrigation water (Pessarakli, 2011). Although GLY is the most widely applied herbicide worldwide, comprehensive knowledge regarding its phytotoxicity to non-target species, such as crops, due to residual soil contamination, is still limited. Recently, our research group provided important clues concerning GLY effects on tomato plants, clearly showing that GLY residues in the soil cause oxidative stress, severely compromising plant growth after 28 days of exposure (Soares et al., 2019a). In this line, the present work is a follow-up study and firstly aimed to unravel the effect of GLY added to the soil on photosynthesis in non-target plants, using *S. lycopersicum* as model species for crops. Although the direct effects of foliar GLY application on the photosynthetic metabolism of target and resistant plants are relatively well described (reviewed by Gomes et al. (2014)), studies exploring changes in the photosynthetic metabolism in response to soil contamination by GLY are still scarce, especially in non-target plants, where agricultural crops are included, and for which it is of utmost importance to assess the potential impacts on yield.

4.1. The presence of GLY residues in the soil ended up affecting the subcellular organization of tomato leaves, promoting an increase of cell death

Although it is claimed that GLY in the soil should not represent a risk to non-target plants (http://www.glyphosate.eu/glyphosate-safety-profile-non-target-wildlife-and-plants), growing evidence has been showing the opposite for different species, such as barley (*Hordeum vulgare* L.), willow (*Salix miyabeana*), saltmarsh bulrush (*Bolboschoenus maritimus* L.), pea (*Pisum sativum* L.) and even tomato (*S. lycopersicum* L.) (Soares et al., 2019a; Gomes et al., 2017; Spormann et al., 2019; Gomes et al., 2016a; Singh et al., 2017; Mateos-Naranjo and Perez-Martin, 2013). In line with this, and corroborating our previous work (Soares et al., 2019a), the exposure of tomato plants to increased concentrations of the herbicide resulted in a substantial alteration of leaf morphology and shape (Fig. 3), greatly impairing leaf development. This GLY-induced alterations in leaf architecture were previously reported in *Eucalyptus* sp. and *Arachis hypogaea* L. (peanut) plants, even though in these studies the herbicide was sprayed onto the foliage (Radwan and Fayez, 2016; Tuffi Santos et al., 2009). As reviewed by Sukhov et al. (2019), abiotic stressors, such as contaminants and drought, are able to generate different signals that can reach other parts of the plant, triggering systemic physiological adjustments. Thus, the observed effects on leaves' physiological, biochemical and molecular status, can arise due to the production, at the root level, of hydraulic, chemical and/or electric signals, which then may propagate inducing alterations in leaves. However, knowing that GLY is phloem-mobile, direct consequences of GLY on leaves, derived from its translocation to the aerial organs, are most likely occurring. Based on the interference of GLY with shikimate pathway, it can be suggested that the observed

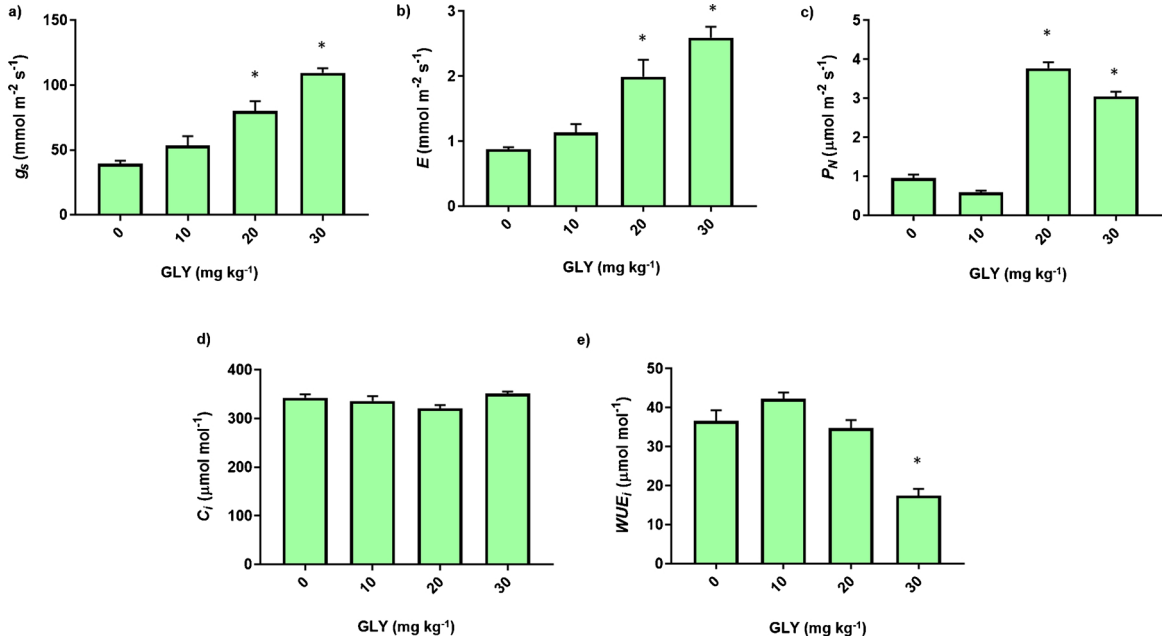

Fig. 10. Stomatal conductance (g_s; a), transpiration (E; b), net CO_2 assimilation (P_N; c) intracellular concentration of CO_2 (Ci; d), water use efficiency ($WUE_i - P_N/G_s$; e) in leaves of *S. lycopersicum* plants exposed to increased concentrations (0, 10, 20 and 30 mg kg^{-1}) of GLY. *Above bars indicate differences from the CTL (0 mg kg^{-1}) at $p \leq 0.05$.

phytotoxicity is a direct consequence of blocking aromatic amino acid and protein synthesis, as evidenced by our results (Fig. 1c–d). In addition to the macroscopic symptoms, GLY exposure also resulted in substantial changes in leaf ultrastructure, especially in what regards to chloroplast organization and structure (Figs. 5 and 6), and in a concentration-dependent manner. Paired with our observations, Vannini et al. (2016) also reported that GLY promoted the occurrence of ultrastructural disturbances in the lichen *Xanthoria parietina* L., when the herbicide was applied to the nutrient solution. Upon GLY treatment, a growing damage of chloroplast integrity was observed, particularly in thylakoid system organization, being this effect accompanied by a rise of PG. According to different studies, these lipoprotein bodies tend to accumulate under stressful conditions, contributing to less damage of cellular sun-structures and to restriction of leaf surface injury (Almeida et al., 2005). Their existence is generally indicative of a high metabolic activity in the chloroplast, being often associated with stress responses and with thylakoid breakdown, but also with senescence events (van Wijk and Kessler, 2017). Moreover, the observed changes in PG number and size in GLY-exposed plants may reflect the metabolic network established between PG and thylakoids, as well as the synthesis of metabolites, such as quinones and tocopherols (van Wijk and Kessler, 2017), which are powerful antioxidants in plant cells (Soares et al., 2019b). This hypothesis makes even more sense considering the results obtained in our previous recent study, where shoots of GLY-treated tomato plants exhibited a prompt and efficient response of the antioxidant (AOX) system, limiting the peroxidation of lipids and the accumulation of reactive oxygen species (ROS) (Soares et al., 2019a). Supporting this, a higher abundance of peroxisomes with paracrystalline inclusions, indicative of catalase (CAT; EC 1.11.1.6) presence (Frederick and Newcomb, 1969), was observed in plants exposed to the highest GLY concentration (Fig. 6a, b, d). Additionally, the maintenance of mitochondria integrity as well as an increased number of mitochondria in leaves of GLY-treated plants (Fig. 6c) can also reflect the high energy demand of these plants to counteract the negative effects of the herbicide. Despite of that, the histochemical detection of cell death unequivocally indicated that GLY ends up hampering cellular homeostasis, inducing cell death in tomato leaves, especially under the highest concentrations tested (20 and 30 mg kg^{-1}). Furthermore, as can be observed in Fig. 6b, some mesophyll cells from plants grown under 30 mg kg^{-1} were severely damaged, as evidenced by the generalized appearance of numerous vesicles throughout the cell and organelles. Based on this set of results, and in order to infer how these structural changes were related to the photosynthetic function, additional studies were designed to evaluate GLY's effects on different biochemical and molecular attributes, as well as on photochemical and gas exchange parameters.

4.2. GLY-induced reduction of D1, CP47 and RuBisCO genes transcription and pigment levels does not inhibit photochemical reactions of photosynthesis

Photosynthesis begins with the absorption of sunlight energy by photosynthetic antenna pigments localized in the thylakoids (Taiz et al., 2015). Thus, stress conditions leading to variations in the content of chlorophylls and carotenoids may induce negative effects in photosynthesis, obstructing the first step of the whole process (Zhong et al., 2018). Either due to its chelating properties or by decreasing Mg content in plant leaves (Cakmak et al., 2009), one of the indirect effects of GLY on photosynthesis is the inhibition of photosynthetic pigments' biosynthesis (Gomes et al., 2014). From our observations, GLY only led to significant reductions in total chlorophylls and carotenoids under the highest concentration applied. Although quite surprising, this phenomenon may be ascribed to two complementary hypotheses, one related to GLY's application mode (soil vs foliar), and the other associated with a low production of AMPA, a metabolite derived from GLY's degradation. Accordingly, GLY primary effects on photosynthesis are directly linked to AMPA, and so, being dependent on the degradation rate of GLY (Reddy et al., 2004; Serra et al., 2013). Due to chemical similarities with glycine, AMPA competes with this amino acid, resulting in decreased levels of δ-aminolevulinic acid, an intermediate in chlorophyll biosynthesis (Gomes et al., 2014). In this sense, it can be suggested that, either by the use of a soil with poor microbial activity, as is the case of the artificial OECD soil used and/or by the root application of GLY, only the highest concentration tested (30 mg kg^{-1}) allowed the production of enough AMPA to inhibit chlorophyll biosynthesis. This observation is further supported by the higher number of PG recorded in plants grown under 30 mg kg^{-1}, since it is known that these lipid bodies play a role in chlorophyll degradation (van Wijk and Kessler, 2017).

After pigment excitation by light in the antenna, the energy is transferred to the reaction centers of PSI and PSII, which is used to channel electrons to the electron transport chain (Taiz et al., 2015). Structurally, the PSII reaction center includes two monomeric core reaction center proteins (D1 and D2), two antenna proteins (CP43 and CP47), two cytochromes, an oxygen evolution protein (PsbO), as well as chlorophyll *a* and other co-factors (Taiz et al., 2015). Thus, transcripts accumulation pattern related to these proteins may provide important hints concerning the response of PSII to GLY exposure. Results of the present study revealed a severe downregulation of both *D1* and *CP47* gene expression in a dose-dependent manner, strongly indicating that, at least transcriptionally, GLY is impairing the normal functioning of PSII. Indeed, since D1 and CP47 are essential for pigments binding and act in energy transfer to the reaction center, respectively (Taiz et al., 2015), changes in their transcript levels may result in disturbances during the photochemical reactions of photosynthesis (Gomes et al., 2014). Thus, it can be assumed that, in addition to affecting protein abundance in PSII by impairing amino acid biosynthesis (Gomes et al., 2014), GLY is also capable of reducing gene expression of PSII-related proteins.

Chlorophyll fluorescence measurements can provide quantitative data related to all stages of the photochemical phase of photosynthesis (Kalaji et al., 2016). Thus, after assessing GLY effects on biochemical and molecular endpoints targeted to PSII, it was decided to take a closer look at the photochemical efficiency of tomato plants exposed to GLY. Despite the negative influence of GLY on the levels of chlorophylls, no apparent effects were observed regarding photochemical parameters. Actually, when plants were exposed to light intensities similar to those experienced during growth, the values of ΦPSII and rETR were increased in response to GLY treatments, suggesting that the observed decrease in chlorophyll content, as well as the depletion of gene expression of D1 and CP47, did not result in photochemical damage, at least under these conditions. Although the rETR (rETR = ΦPSII × PPFD) does not reflect the absolute electron flow across thylakoids membrane, this formula has been widely used in stress physiology studies to report the electron transport rate occurring at a given light intensity in different photoautotrophic organisms and types of samples (Garrido et al., 2019; Masojídek et al., 2001; Ritchie, 2012; Williams et al., 2009; Zivcak et al., 2013), and more specifically on studies dealing with effects of GLY on photosynthesis (Gomes et al., 2017; Yanniccari et al., 2012; Zobiole et al., 2010a; Gomes et al., 2016b; Vital et al., 2017). Besides, even if it is conceivable that GLY, as other stress signals (Sukhova et al., 2018), could have affected p (fraction of PPFD absorbed by leaves) and dII (multiplication factor since the transport of a single electron requires the absorption of two photons), ETR is largely determined by ΦPSII (Genty et al., 1989). Therefore, the results obtained in the current study still translate a significant impact of GLY in the electron transport rate. Although GLY exposure was found to inhibit PSII efficiency, ETR and non-photochemical energy dissipation (see review by Gomes et al. (2014)), it should be stressed out that the majority of those studies evaluated the effects of GLY foliar application in resistant/susceptible plants. However, Cañero et al. (2011) and Gravena et al. (2012) (2009) also observed no negative signs on

fluorescence parameters in olive and citrus plants, both considered as non-target species, upon exposure to GLY. Furthermore, in the present study, an inverse relationship between photochemical efficiency and non-photochemical quenching was observed, as revealed by the higher rETR and ΦPSII, and lower NPQ levels. Indeed, although NPQ plays an important role in energy dissipation under excessive light conditions (Ruban, 2016), it may be suggested that, under growing light conditions, plants exposed to the herbicide increased their photochemical efficiency, allowing more power to be rerouted to the PSII and, thus, decreasing the NPQ. In an attempt to confirm the results obtained, an assay towards the evaluation of photochemical recovery upon exposure to high light saturating conditions for 1 h was performed. In fact, while the fluorescence photochemical parameters (e.g. F_v/F_m and ΦPSII) may bring useful information regarding photosynthetic responses under steady-state, PSII photoinactivation and photorepair studies are of utmost importance to the proper understanding of photosynthetic responses to light (Serôdio et al., 2017) and references therein). Upon exposure to high light conditions, plants need to employ distinct compensatory mechanisms to control the excessive energy not used for photochemistry. One of the most common pathways is the non-photochemical quenching (NPQ), which transforms excitation energy into heat, contributing to a lower production of singlet oxygen ($^1O_2$) and preventing photo-oxidative stress in chloroplasts (Ruban, 2016). NPQ is a complex mechanism that comprises, at least, three different components—qE (energy dependent component), qT (redistribution of energy from PSII to PSI) and qI (photoinhibition) (Latowski et al., 2011). The major NPQ component, qE, starts after the activation of the PsbS protein and the xanthophyll cycle, in which violaxanthin is reversibly converted into zeaxanthin, in response to the acidification of thylakoid lumen caused by the operation of the electron transport chain (Ruban, 2016; Latowski et al., 2011). Chemically, xanthophylls belong to the group of the carotenoids, which are recognized as important AOX especially in light stress conditions (Soares et al., 2019b). Thus, knowing that carotenoid and NPQ levels were decreased in response to the herbicide, GLY-treated plants were expected to present a lower photochemical recovery rate. However, as can be observed in Fig. 9, plants exposed to increased concentrations of GLY showed a better photochemical recovery after high light saturating conditions. Moreover, although all groups of plants recover faster within the first few minutes (Fig. 9), only the plants exposed to the highest GLY concentrations (20 and 30 mg kg^{-1}) continue to recover, reaching values closer to 90% of the initial value. This behavior supports the hypothesis that NPQ, through the activation of the xanthophyll cycle, is not the only mechanism underlying the higher photochemical recovery in GLY-stressed plants. Indeed, it is recognized that NPQ related to the xanthophyll cycle (qE) relaxes within few minutes (≈5 min) (Ruban, 2016), so there must be other mechanisms to balance the observed decrease in chlorophylls levels and D1 and CP47 transcripts. Indeed, it seems that cells tried to overcome GLY-induced stress by triggering offsetting mechanisms at the expense of a high energy demand (evidenced by the higher abundance of mitochondria). As recently reported, GLY application resulted in a higher efficient response of the plant's AOX system, enhancing the levels of proline and the main AOX enzymes, including ascorbate peroxidase (APX; EC 1.11.1.11) and CAT; (Soares et al., 2019a). Thus, it appears that, under GLY exposure, the prompt response of the plant's AOX system helped to mitigate and/or reverse any photooxidative damage, resulting in a higher recovery date but also explaining the higher photochemical efficiencies of GLY-treated plants. In order to pursuit this hypothesis, further experiments will be designed to quantify the total AOX capacity right before and after the saturating light period.

Overall, based on our results, it can be hypothesized that, although GLY greatly impaired photosynthetic metabolism at the transcriptional and biochemical level, the cells were able to activate compensatory mechanisms, which is demonstrated by the stimulation of the photochemical reactions and by the higher energy demand related to the increased number of mitochondria. Despite of that, it should be stressed that the substantial investment of cellular energy in protective mechanisms (NPQ and/or AOX defenses) to maintain the photochemical efficiency, ends up dysregulating the normal plant metabolism, possibly resulting in a higher cell death and damaging the ultrastructure of tomato leaves, thereby compromising plant growth.

4.3. GLY exposure does not compromise the photosynthetic CO_2 fixation or photosynthesis, but results in reduced water use efficiency (WUE)

It is well documented that foliar-applied GLY substantially reduces the chemical yield of photosynthesis, by promoting the malfunctioning of stomata (Gomes et al., 2014). However, no study has elucidated the connection between root-applied GLY and the performance of photosynthetic CO_2 fixation yet. Somewhat unexpectedly, our results showed that the herbicide not only did not apparently hamper this mechanism but instead promotes a 3−4-fold increment in CO_2 fixation in plants treated with the two highest GLY concentrations (20 and 30 mg kg^{-1}). Although this might seem a little surprising, these observations are somewhat in line with the results relative to the photochemical efficiency. Nevertheless, transcript levels and RuBisCO content were reduced upon exposure to GLY, corroborating the observations of previous studies (Servaites et al., 1987), especially at the highest GLY concentration (Fig. 7b). These findings reinforce the premise that the herbicide is affecting subcellular homeostasis at both transcriptional and protein levels, which would probably reflect in a decrease of Calvin cycle yield if the exposure period was longer.

Although our results have shown that exposure to increasing GLY concentrations also resulted in proportionally higher stomatal conductance, at least partially explaining the unexpected increment in P_N, the response of P_N to GLY concentration was not dose-dependent (Fig. 10a, c), suggesting that factors other than stomata limitations are governing the measured photosynthetic activity. As can be observed (Fig. 10c), although plants under 30 mg kg^{-1} exhibited a higher C assimilation rate than the CTL, the observed increase was lower than that of plants under 20 mg kg^{-1}. Probably, this phenomenon can be explained by biochemical limitations rather than diffusional ones, perhaps by an impact on RuBisCO content (Fig. 1d) and expression (Fig. 7b). From what it appears, upon exposure to the highest GLY concentration, the registered inhibition on RuBisCO gene expression and protein content is already impacting the CO_2 assimilation, whose levels were closer to the ones of the CTL. Thus, it can be suggested that, although the intracellular concentration of CO_2 did not change, a lower content of RuBisCO transcripts and polypeptides did not allow the further increase of CO_2 assimilation rate. Moreover, our findings also suggest that, at the highest tested concentration, GLY may compromise plant water balance, since *WUEi* was strongly diminished (Fig. 10e), what may further impact on photosynthetic activity. In fact, according to Zobiole et al. (2010b), the application of different GLY rates to GLY-resistant soybean plants ends up blocking the water uptake, reducing the WUE. On the other hand, knowing that the CO_2 fixation rate is expressed per unit leaf area (μmol m^{-2} s^{-1}), the sharp increment in P_N of plants exposed to GLY at 20 and 30 mg kg^{-1} when compared to those in CTL, not paralleled by g_s, can also be explained by the alteration on leaf mesophyll structure caused by GLY treatment, as can be observed by the significant reduction in SLA at those highest GLY concentration (Fig. 3c).

Although the interdependence of photosynthetic reactions is unquestionable, it is recognized that the photochemical and chemical phases can be differentially affected by abiotic stress factors (Sharma et al., 2019). Thus, in order to better understand the chain of photosynthetic events affected by GLY, correlation analyses between multiple parameters, namely between components of the two phases of photosynthesis, were performed. Although it was not always possible to find significant correlations, namely when rETR and P_N values were plotted ($p > 0.05$; Supplementary Material), it should be noted that, when

integrating NPQ and P_N values, the rate of CO_2 assimilation increased, as the energy dissipated in the form of heat decreased (< NPQ), especially in plants treated with GLY. However, for the same NPQ value, plants exposed to 20 mg kg^{-1} show a greater assimilation potential than those treated with 30 mg kg^{-1}. In what concerns the gas-exchange parameters, significant correlations ($p < 0.05$; Supplementary Material) were detected between E and P_N. This observation, together with the relationship found between NPQ and P_N, sustains the hypothesis previously raised: the lower CO_2 assimilation rate of plants exposed to the highest concentration (30 mg kg^{-1}), in relation to those exposed to 20 mg kg^{-1}, is not due to stomatal restrictions, but most probably to biochemical and molecular limitations, contributing for a lower water use efficiency.

So, studies must consider the alterations caused by GLY treatment, from the subcellular to the physiological level, to have a more realistic picture of the impact at the plant level. Furthermore, the higher values of stomatal conductance and transpiration induced by GLY can clearly affect water relations in the plant, raising its water requirements. Thus, from an agronomic perspective, this can be regarded as an important indirect effect of GLY on crops, which can bring important economic issues and must be carefully analyzed.

5. Main conclusions

The results obtained in the current study helped to disclose the consequences of soil contamination by GLY in the photosynthetic performance of one of the main crops worldwide, *S. lycopersicum*. The combination of ecophysiological, ultrastructural, biochemical and molecular tools allowed to achieve a robust and comprehensive perception of the mechanisms behind GLY-induced stress in plants. From a wide perspective, it can be concluded that, although growth and development of this species is highly compromised by the herbicide exposure (Soares et al., 2019a), the observed toxicity in leaf ultrastructure, cell viability and water use efficiency, as well as in the transcriptional and biochemical control of photosynthetic-related players, seems not to substantially reduce carbon flow through photosynthesis, at least in a short-term exposure. Based on previous findings from our group, this apparent maintenance of photosynthesis is probably related to the stimulation of the AOX defenses (Soares et al., 2019a), which must have been efficient at preventing ROS-induced damage in the viable cells of leaf mesophyll, and also closely related to a higher energetic investment to ensure the homeostasis of the cells. Thus, we hope that this work motivates future research efforts to clearly understand the risks of GLY overuse in non-target crops, not only from a productivity point-of-view, but also focusing on metabolic events which may help to develop ways to minimize GLY toxicity.

CRediT authorship contribution statement

Cristiano Soares: Conceptualization, Formal analysis, Investigation, Methodology, Writing - original draft, Writing - review & editing. **Ruth Pereira:** Conceptualization, Funding acquisition, Project administration, Resources, Supervision, Validation, Writing - review & editing. **Maria Martins:** Methodology, Investigation. **Paula Tamagnini:** Funding acquisition, Resources. **João Serôdio:** Investigation, Methodology, Writing - review & editing. **José Moutinho-Pereira:** Investigation, Methodology, Writing - review & editing. **Ana Cunha:** Conceptualization, Supervision, Validation, Writing - review & editing, Methodology. **Fernanda Fidalgo:** Conceptualization, Funding acquisition, Project administration, Resources, Supervision, Validation, Writing - review & editing.

Declaration of Competing Interest

The authors declare that they have no known competing financial interests or personal relationships that could have appeared to influence the work reported in this paper.

Acknowledgments

The authors would like to acknowledge GreenUPorto (FCUP) for financial and equipment support and Foundation for Science and Technology (FCT) for providing a PhD scholarship to C. Soares (SFRH/BD/115643/2016). This research was also supported by national funds, through FCT/MCTES, within the scope of UIDB/05748/2020 and UIDP/05748/2020 (GreenUPorto), and UIDP/50017/2020 and UIDB/50017/2020 (CESAM). The authors gratefully acknowledge the valuable assistance of Dr. Rui Fernandes and Dr. Ana Rita Malheiro in the ultrastructural analysis.

Appendix A. Supplementary data

Supplementary material related to this article can be found, in the online version, at doi:https://doi.org/10.1016/j.jhazmat.2020.122871.

References

Almeida, J.M., Fidalgo, F., Confraria, A., Santos, A., Pires, H., Santos, I., 2005. Effect of hydrogen peroxide on catalase gene expression, isoform activities and levels in leaves of potato sprayed with homobrassinolide and ultrastructural changes in mesophyll cells. Funct. Plant Biol. 32, 707–720. https://doi.org/10.1071/FP04235.

Atwood, D., Paisley-Jones, C., 2017. Pesticides Industry Sales and Usage. 2008–2012 Market Estimates. Washington, DC, USA. .

Bai, S.H., Ogbourne, S.M., 2016. Glyphosate: environmental contamination, toxicity and potential risks to human health via food contamination. Environ. Sci. Pollut. Res. 23, 18988–19001. https://doi.org/10.1007/s11356-016-7425-3.

Borggaard, O.K., Gimsing, A.L., 2008. Fate of glyphosate in soil and the possibility of leaching to ground and surface waters: a review. Pest Manag. Sci. 64, 441–456. https://doi.org/10.1002/ps.1512.

Bradford, M.M., 1976. Rapid and sensitive method for quantitation of microgram quantities of protein utilizing principle of protein-dye binding. Anal. Biochem. 72, 248–254. https://doi.org/10.1006/abio.1976.9999.

Branco-Neves, S., Soares, C., de Sousa, A., Martins, V., Azenha, M., Gerós, H., Fidalgo, F., 2017. An efficient antioxidant system and heavy metal exclusion from leaves make *Solanum cheesmaniae* more tolerant to Cu than its cultivated counterpart. Food Energy Secur. 6, 123–133. https://doi.org/10.1002/fes3.114.

Cakmak, I., Yazici, A., Tutus, Y., Ozturk, L., 2009. Glyphosate reduced seed and leaf concentrations of calcium, manganese, magnesium, and iron in non-glyphosate resistant soybean. Eur. J. Agron. 31, 114–119.

Cañero, A.I., Cox, L., Redondo-Gómez, S., Mateos-Naranjo, E., Hermosín, M.C., Cornejo, J., 2011. Effect of the herbicides terbuthylazine and glyphosate on photosystem II photochemistry of young olive (*Olea europaea*) plants. J. Agric. Food Chem. 59, 5528–5534. https://doi.org/10.1021/jf200875u.

Costa, L., Primost, J.E., Carriquiriborde, P., 2017. Glyphosate and AMPA, "pseudo-persistent" pollutants under real- world agricultural management practices in the Mesopotamic Pampas agroecosystem, Argentina. Environ Pollut 229, 771–779. https://doi.org/10.1016/j.envpol.2017.06.006.

Dorais, M., Ehret, D.L., Papadopoulos, A.P., 2008. Tomato (*Solanum lycopersicum*) health components: from the seed to the consumer. Phytochem. Rev. 7, 231–250. https://doi.org/10.1007/s11101-007-9085-x.

Dzakovich, M.P., Ferruzzi, M.G., Mitchell, C.A., 2016. Manipulating sensory and phytochemical profiles of greenhouse tomatoes using environmentally relevant doses of ultraviolet radiation. J. Agric. Food Chem. 64 (36), 6801–6808.

EPA, 2017. Revised Glyphosate Issue Paper: Evaluation of Carcinogenic Potential. (Accessed 30 July 2019). https://cfpub.epa.gov/si/si_public_record_Report.cfm?Lab=OPP&dirEntryId=337935.

Franz, J.E., Mao, M.K., Sikorski, J.A., 1997. Glyphosate: a Unique Global Herbicide. American Chemical Society.

Frederick, S.E., Newcomb, E.H., 1969. Cytochemical localization of catalase in leaf microbodies (peroxisomes). J. Cell Biol. 43, 343–353. https://doi.org/10.1083/jcb.43.2.343.

Garrido, A., Serôdio, J., De Vos, R., Conde, A., Cunha, A., 2019. Influence of foliar kaolin application and irrigation on photosynthetic activity of grape berries. Agronomy 9, 685. https://doi.org/10.3390/agronomy9110685.

Genty, B., Briantais, J.-M., Baker, N.R., 1989. The relationship between the quantum yield of photosynthetic electron transport and quenching of chlorophyll fluorescence. Biochim. Biophys. Acta - Gen. Subj. 990, 87–92. https://doi.org/10.1016/S0304-4165(89)80016-9.

Gerszberg, A., Hnatuszko-Konka, K., Kowalczyk, T., Kononowicz, A.K., 2015. Tomato (*Solanum lycopersicum* L.) in the service of biotechnology. Plant Cell Tissue Organ Cult. 120, 881–902. https://doi.org/10.1007/s11240-014-0664-4.

Gomes, M.P., Smedbol, E., Chalifour, A., Hénault-Ethier, L., Labrecque, M., Lepage, L., Lucotte, M., Juneau, P., 2014. Alteration of plant physiology by glyphosate and its by-product aminomethylphosphonic acid: an overview. J. Exp. Bot. 65, 4691–4703. https://doi.org/10.1093/jxb/eru269.

Gomes, M.P., Le Manac'h, S.G., Moingt, M., Smedbol, E., Paquet, S., Labrecque, M., Lucotte, M., Juneau, P., 2016a. Impact of phosphate on glyphosate uptake and toxicity in willow. J. Hazard. Mater. 304, 269–279. https://doi.org/10.1016/j.jhazmat.2015.10.043.

Gomes, M.P., Le Manac'h, S.G., Maccario, S., Labrecque, M., Lucotte, M., Juneau, P., 2016b. Differential effects of glyphosate and aminomethylphosphonic acid (AMPA) on photosynthesis and chlorophyll metabolism in willow plants. Pestic. Biochem. Physiol. 130, 65–70. https://doi.org/10.1016/j.pestbp.2015.11.010.

Gomes, M.P., Le Manac'h, S.G., Hénault-Ethier, L., Labrecque, M., Lucotte, M., Juneau, P., 2017. Glyphosate-dependent inhibition of photosynthesis in willow. Front. Plant Sci. 8, 207. https://doi.org/10.3389/fpls.2017.00207.

Gravena, R., Filho, R.V., Alves, P.L.C.A., Mazzafera, P., Gravena, A.R., 2009. Low glyphosate rates do not affect *Citrus limonia* (L.) Osbeck seedlings. Pest Manag. Sci. 65, 420–425. https://doi.org/10.1002/ps.1694.

Gravena, R., Filho, R.V., Alves, P.L.C.A., Mazzafera, P., Gravena, A.R., 2012. Glyphosate has low toxicity to citrus plants growing in the field. Can. J. Plant Sci. 92, 119–127. https://doi.org/10.4141/cjps2011-055.

Kalaji, H.M., Jajoo, A., Oukarroum, A., Brestic, M., Zivcak, M., Samborska, I.A., Cetner, M.D., Łukasik, I., Goltsev, V., Ladle, R.J., 2016. Chlorophyll a fluorescence as a tool to monitor physiological status of plants under abiotic stress conditions. Acta Physiol. Plant. 38, 102. https://doi.org/10.1007/s11738-016-2113-y.

Kitajima, M., Butler, W.L., 1975. Quenching of chlorophyll fluorescence and primary photochemistry in chloroplasts by dibromothymoquinone. Biochim. Biophys. Acta - Bioenerg. 376, 105–115. https://doi.org/10.1016/0005-2728(75)90209-1.

Latowski, D., Kuczyńska, P., Strzałka, K., 2011. Xanthophyll cycle – a mechanism protecting plants against oxidative stress. Redox Rep. 16, 78–90. https://doi.org/10.1179/174329211X13020951739938.

Leclercq, J., Adams-Phillips, L.C., Zegzouti, H., Jones, B., Latché, A., Giovannoni, J.J., Pech, J.-C., Bouzayen, M., 2002. LeCTR1, a tomato CTR1-like gene, demonstrates ethylene signaling ability in arabidopsis and novel expression patterns in tomato. Plant Physiol. 130, 1132–1142. https://doi.org/10.1104/pp.009415.

Li, Y., Ren, B., Ding, L., Shen, Q., Peng, S., Guo, S., 2013. Does chloroplast size influence photosynthetic nitrogen use efficiency? PLoS One 8, e62036. https://doi.org/10.1371/journal.pone.0062036.

Lichtenthaler, H.K., 1987. Chlorophylls and carotenoids - pigments of photosynthetic BIOMEMBRANES. Methods Enzymol. 148, 350–382.

Livak, K.J., Schmittgen, T.D., 2001. Analysis of relative gene expression data using real-time quantitative PCR and the $2^{-\Delta\Delta CT}$ method. Methods 25, 402–408.

Løvdal, T., Lillo, C., 2009. Reference gene selection for quantitative real-time PCR normalization in tomato subjected to nitrogen, cold, and light stress. Anal. Biochem. 387, 238–242. https://doi.org/10.1016/j.ab.2009.01.024.

Mariz-Ponte, N., 2017. Use of the UV-A and UV-B Light Supplementation in Tomato Producing: a Perspective From Plant to Fruit. Faculty of Sciences of University of Porto, Porto. https://repositorio-aberto.up.pt/handle/10216/110653.

Masojídek, J., Grobbelaar, J.U., Pechar, L., KoblížEk, M., 2001. Photosystem II electron transport rates and oxygen production in natural waterblooms of freshwater cyanobacteria during a diel cycle. J. Plankton Res. 23, 57–66.

Mateos-Naranjo, E., Perez-Martin, A., 2013. Effects of sub-lethal glyphosate concentrations on growth and photosynthetic performance of non-target species *Bolboschoenus maritimus*. Chemosphere 93, 2631–2638. https://doi.org/10.1016/j.chemosphere.2013.09.094.

Mateos-Naranjo, E., Redondo-Gómez, S., Cox, L., Cornejo, J., Figueroa, M.E., 2009. Effectiveness of glyphosate and imazamox on the control of the invasive cordgrass Spartina densiflora. Ecotoxicol. Environ. Saf. 72, 1694–1700. https://doi.org/10.1016/J.ECOENV.2009.06.003.

Murashige, T., Skoog, F., 1962. A revised medium for rapid growth and bio assays with tobacco tissue cultures. Physiol. Plant. 15, 473–497.

OECD, 2006. Test No. 208: Terrestrial Plant Test: Seedling Emergence and Seedling Growth Test. OECD Publishing. file:///content/book/9789264070066-en.

Parween, T., Jan, S., Mahmooduzzafar, S., Fatma, T., Siddiqui, Z.H., 2016. Selective effect of pesticides on plant—a review. Crit. Rev. Food Sci. Nutr. 56, 160–179. https://doi.org/10.1080/10408398.2013.787969.

Peruzzo, P.J., Porta, A.A., Ronco, A.E., 2008. Levels of glyphosate in surface waters, sediments and soils associated with direct sowing soybean cultivation in north pampasic region of Argentina. Environ. Pollut. 156, 61–66. https://doi.org/10.1016/j.envpol.2008.01.015.

Pessarakli, M., 2011. Handbook of Plant and Crop Stress. CRC Press (Accessed 3 July 2019). https://www.crcpress.com/Handbook-of-Plant-and-Crop-Stress/Pessarakli/p/book/9781439813966.

Radwan, D.E.M., Fayez, K.A., 2016. Photosynthesis, antioxidant status and gas-exchange are altered by glyphosate application in peanut leaves. Photosynthetica 54, 307–316. https://doi.org/10.1007/s11099-016-0075-3.

Reddy, K.N., Rimando, A.M., Duke, S.O., 2004. Aminomethylphosphonic acid, a metabolite of glyphosate, causes injury in glyphosate-treated, glyphosate-resistant soybean. J. Agric. Food Chem. 52, 5139–5143. https://doi.org/10.1021/jf049605v.

Ritchie, R.J., 2012. Photosynthesis in the blue water lily (*nymphaea caerulea* saligny) using pulse amplitude modulation fluorometry. Int. J. Plant Sci. 173, 124–136. https://doi.org/10.1086/663168.

Ruban, A.V., 2016. Nonphotochemical chlorophyll fluorescence quenching: mechanism and effectiveness in protecting plants from Photodamage. Plant Physiol. 170, 1903–1916. https://doi.org/10.1104/pp.15.01935.

Serôdio, J., Schmidt, W., Frankenbach, S., 2017. A chlorophyll fluorescence-based method for the integrated characterization of the photophysiological response to light stress. J. Exp. Bot. 68, erw492. https://doi.org/10.1093/jxb/erw492.

Serra, A.-A., Nuttens, A., Larvor, V., Renault, D., Couée, I., Sulmon, C., Gouesbet, G., 2013. Low environmentally relevant levels of bioactive xenobiotics and associated degradation products cause cryptic perturbations of metabolism and molecular stress responses in *Arabidopsis thaliana*. J. Exp. Bot. 64, 2753–2766. https://doi.org/10.1093/jxb/ert119.

Servaites, J.C., Tucci, M.A., Geiger, D.R., 1987. Glyphosate effects on carbon assimilation, ribulose bisphosphate carboxylase activity, and metabolite levels in sugar beet leaves. Plant Physiol. 85, 370–374. https://doi.org/10.2307/4270917.

Sharma, A., Kumar, V., Kumar, R., Shahzad, B., Thukral, A.K., Bhardwaj, R., 2018. Brassinosteroid - mediated pesticide detoxification in plants : a mini - review. Cogent Food Agric. 4, 1436212. https://doi.org/10.1080/23311932.2018.1436212.

Sharma, A., Kumar, V., Shahzad, B., Ramakrishnan, M., Sidhu, G.P.S., Bali, A.S., Handa, N., Kapoor, D., Yadav, P., Khanna, K., 2019. Photosynthetic response of plants under different abiotic stresses: a review. J. Plant Growth Regul. 1–23.

Silva, V., Montanarella, L., Jones, A., Fernández-ugalde, O., Mol, H.G.J., Ritsema, C.J., Geissen, V., 2018. Science of the total environment distribution of glyphosate and aminomethylphosphonic acid (AMPA) in agricultural topsoils of the European Union. Sci. Total Environ. 621, 1352–1359. https://doi.org/10.1016/j.scitotenv.2017.10.093.

Singh, H., Singh, N.B., Singh, A., Hussain, I., Singh, H., Singh, N.B., Singh, A., Hussain, I., 2017. Exogenous application of salicylic acid to alleviate glyphosate stress in *Solanum lycopersicum*. Int. J. Veg. Sci. 23, 552–566. https://doi.org/10.1080/19315260.2017.1347845.

Soares, C., Branco-Neves, S., de Sousa, A., Pereira, R., Fidalgo, F., 2016a. Ecotoxicological relevance of nano-NiO and acetaminophen to *Hordeum vulgare* L.: combining standardized procedures and physiological endpoints. Chemosphere 165, 442–452. https://doi.org/10.1016/j.chemosphere.2016.09.053.

Soares, C., de Sousa, A., Pinto, A., Azenha, M., Teixeira, J., Azevedo, R.A., Fidalgo, F., 2016b. Effect of 24-epibrassinolide on ROS content, antioxidant system, lipid peroxidation and Ni uptake in *Solanum nigrum* L. Under Ni stress. Environ. Exp. Bot. 122, 115–125. https://doi.org/10.1016/j.envexpbot.2015.09.010.

Soares, C., Pereira, R., Spormann, S., Fidalgo, F., 2019a. Is soil contamination by a glyphosate commercial formulation truly harmless to non-target plants? – evaluation of oxidative damage and antioxidant responses in tomato. Environ. Pollut. 247, 256–265. https://doi.org/10.1016/j.envpol.2019.01.063.

Soares, C., Carvalho, M.E.A., Azevedo, R.A., Fidalgo, F., 2019b. Plants facing oxidative challenges—a little help from the antioxidant networks. Environ. Exp. Bot. 161, 4–25. https://doi.org/10.1016/J.ENVEXPBOT.2018.12.009.

Spormann, S., Soares, C., Fidalgo, F., 2019. Salicylic acid alleviates glyphosate-induced oxidative stress in *Hordeum vulgare* L. J. Environ. Manage. 241, 226–234. https://doi.org/10.1016/j.jenvman.2019.04.035.

Sukhova, E., Mudrilov, M., Vodeneev, V., Sukhov, V., 2018. Influence of the variation potential on photosynthetic flows of light energy and electrons in pea. Photosynth. Res. 136 (2), 215–228.

Sukhov, V., Sukhova, E., Vodeneev, V., 2019. Long-distance electrical signals as a link between the local action of stressors and the systemic physiological responses in higher plants. Prog. Biophys. Mol. Biol. 146, 63–84. https://doi.org/10.1016/j.pbiomolbio.2018.11.009.

Taiz, L., Zeiger, E., Moller, I.M., Murphy, A., 2015. Plant Physiology and Development, Sixth. Sinauer Associates, Inc., Sunderland, U.S.A.

Tuffi Santos, L., Sant'Anna-Santos, B., Meira, R., Ferreira, F., Tiburcio, R., Machado, A., 2009. Leaf anatomy and morphometry in three eucalypt clones treated with glyphosate. Brazilian J. Biol. 69, 129–136. https://doi.org/10.1590/S1519-69842009000100016.

Van Bruggen, A.H.C., He, M.M., Shin, K., Mai, V., Jeong, K.C., Finckh, M.R., Morris, J.G., 2018. Environmental and health effects of the herbicide glyphosate. Sci. Total Environ. 616–617, 255–268. https://doi.org/10.1016/j.scitotenv.2017.10.309.

van Wijk, K.J., Kessler, F., 2017. Plastoglobuli: plastid microcompartments with integrated functions in metabolism, plastid developmental transitions, and environmental adaptation. Annu. Rev. Plant Biol. 68, 253–289. https://doi.org/10.1146/annurev-arplant-043015-111737.

Vannini, A., Guarnieri, M., Paoli, L., Sorbo, S., Basile, A., Loppi, S., 2016. Bioaccumulation, physiological and ultrastructural effects of glyphosate in the lichen *Xanthoria parietina* (L.) Th. Fr. Chemosphere 164, 233–240. https://doi.org/10.1016/j.chemosphere.2016.08.058.

Vital, R.G., Jakelaitis, A., Silva, F.B., Batista, P.F., Almeida, G.M., Costa, A.C., Rodrigues, A.A., 2017. Physiological changes and in the carbohydrate content of sunflower plants submitted to sub-doses of glyphosate and trinexapac-ethyl. Bragantia 76, 33–44. https://doi.org/10.1590/1678-4499.540.

von Von Caemmerer, S., Farquhar, G.D., 1981. Some relationships between the biochemistry of photosynthesis and the gas exchange of leaves. Planta 153, 376–387.

Wei, C., Song, L., Yang, W., Zhao, Y., 2016. Research on glyphosate pesticide residue in surface water in Guiyang. Environ. Sci. Technol. 3, 23.

Williams, S.L., Carranza, A., Kunzelman, J., Datta, S., Kuivila, K.M., 2009. Effects of the herbicide diuron on cordgrass (*Spartina foliosa*) reflectance and photosynthetic parameters. Estuaries Coasts 32, 146–157. https://doi.org/10.1007/s12237-008-9114-z.

Yanniccari, M., Tambussi, E., Istilart, C., Castro, A.M., 2012. Glyphosate effects on gas exchange and chlorophyll fluorescence responses of two *Lolium perenne* L. Biotypes with differential herbicide sensitivity. Plant Physiol. Biochem. 57, 210–217. https://doi.org/10.1016/J.PLAPHY.2012.05.027.

Zhang, C., Hu, X., Luo, J., Wu, Z., Wang, L., Li, B., Wang, Y., Sun, G., 2015. Degradation dynamics of glyphosate in different types of citrus orchard soils in China. Molecules 20, 1161–1175. https://doi.org/10.3390/molecules20011161.

Zhong, G., Wu, Z., Yin, J., Chai, L., 2018. Responses of *Hydrilla verticillata* (L.f.) Royle and *Vallisneria natans* (Lour.) Hara to glyphosate exposure. Chemosphere 193, 385–393. https://doi.org/10.1016/j.chemosphere.2017.10.173.

Zivcak, M., Brestic, M., Balatova, Z., Drevenakova, P., Olsovska, K., Kalaji, H.M., Yang, X., Allakhverdiev, S.I., 2013. Photosynthetic electron transport and specific photo-protective responses in wheat leaves under drought stress. Photosynth. Res. 117, 529–546. https://doi.org/10.1007/s11120-013-9885-3.

Zobiole, L.H.S., de Oliveira Jr., R.S., Kremer, R.J., Muniz, A.S., de Oliveira Jr., A., 2010a. Nutrient accumulation and photosynthesis in glyphosate-resistant soybeans is reduced under glyphosate use. J. Plant Nutr. 33, 1860–1873. https://doi.org/10.1080/01904167.2010.491890.

Zobiole, L.H.S., de Oliveira, R.S., Kremer, R.J., Constantin, J., Bonato, C.M., Muniz, A.S., 2010b. Water use efficiency and photosynthesis of glyphosate-resistant soybean as affected by glyphosate. Pestic. Biochem. Physiol. 97, 182–193. https://doi.org/10.1016/J.PESTBP.2010.01.004.

Zobiole, L.H.S., Kremer, R.J., de Oliveira Jr, R.S., Constantin, J., 2012. Glyphosate effects on photosynthesis, nutrient accumulation, and nodulation in glyphosate-resistant soybean. J. Plant Nutr. Soil Sci. (1999) 175, 319–330. https://doi.org/10.1002/jpln.201000434.